

An Entropy Based Model for Velocity-Dip-Position

S. Kundu^{1*} and K. Ghoshal²¹Department of Basic Sciences and Humanities, IIIT Bhubaneswar, Odisha 751 003, India²Department of Mathematics, Indian Institute of Technology Kharagpur, Kharagpur 721302, India

Received 1 Apr 2016; revised 13 August 2016; accepted 26 September 2016; published online 21 December 2016

ABSTRACT. In this study, theoretical models have been developed to predict the velocity-dip-position in steady and uniform turbulent flow through open channels. Unlike the previous works where empirical or semi-empirical models were suggested, the present models are developed from a mathematical approach based on the concept of entropy theory. Considering dimensionless dip-position as a random variable and starting from the Shannon entropy on probability distribution, models are derived by maximizing the entropy function using the principle of maximum entropy. It has been shown that proposed models are applicable over the whole cross section as well as at the central section of any rectangular open channel. The models are validated with a large number of experimental data sets published in literature for a wide variety of flow conditions. Apart from this, the models are also compared with other similar models existing in literature and the prediction accuracy of the present models are confirmed by computing five different errors for all the models. Out of the two proposed models, the model $M2_c$ satisfies the required asymptotic boundary conditions. At the end, model $M2_c$ is expressed in terms of a damping function. The non-occurrence of maximum velocity at the free surface, commonly known as dip-phenomenon, is explained in the light of the proposed damping concept.

Keywords: velocity-dip-phenomenon, Shannon entropy, Lagrange multiplier, least-square technique, open channel turbulent flow

1. Introduction

The vertical velocity profile in a uniform turbulent flow through open channels has drawn the attention of scientists and hydraulic engineers since a long time. The location of the maximum velocity from channel bottom has special interest among civil engineers, geologists, hydrologists and other researchers. For more than a century ago, scientists Francis (1878), Stearns (1883), Murphy (1904), Gibson (1909) and Vanoni (1946) have found the position of the maximum mean velocity below the water surface. This phenomenon is known as velocity-dip-phenomenon and the location of maximum velocity from channel bottom is known as velocity-dip-position. The maximum velocity in an open-channel at any cross section may occur up to 45% of the flow depth below the free surface (Stearns, 1883; Hu and Hui, 1995). Even in the large river like the Mississippi River, the maximum velocity appears at two-third of the water depth from the channel bottom (Gordon, 1992). Moreover, the maximum velocity usually occurs beneath the water surface during flood periods (Gordon, 1992). Many experiments have been conducted to measure the mean velocity profiles along vertical direction in open-channel turbulent flow and it has been observed that at

the central section of an open channel the velocity-dip-phenomenon occurs if the aspect ratio of the channel Ar (defined as the ratio of channel width b to flow depth h) is less than a certain value, called the critical aspect ratio $Ar_c \approx 5$. From their experimental observations, Nezu and Rodi (1985) proposed that $Ar_c \approx 5$. Again, though at the central section of a wide open channel (where $Ar > Ar_c$) maximum velocity appears at the free surface, but near to the sidewall region the dip phenomenon appears (Vanoni, 1941). Vanoni (1941) also suggested that for wide open channels, there always exists a central region where no dip phenomenon occurs. Later on, Nezu and Rodi (1985) found that in the central region $|(b/2 - z)/h| < (Ar - Ar_c)/2$ (where z is distance from the side wall) maximum velocity always observed at the free surface.

It is a challenge to scientists and engineers to predict the velocity-dip-position at any given distance z from sidewall for open channel flows. According to the best of our knowledge, till now no mathematical model has been developed for predicting the dip-position from a theoretical background. Different analytical (empirical or semi-empirical) and numerical models and methods are reported by several investigators time to time. Wang et al. (2001) proposed a relation for y_d (the location of velocity-dip-position from channel bottom or bed) as a function of lateral distance z by observing the pattern of measured data obtained by Nezu and Rodi (1986) and other eight researchers. Their empirical model represents a linear trend of sine wave function and is applicable only to narrow open channels. They also proposed a model for dimensionless dip-position $\xi_d (= y_d/h$, where h is the flow depth) at the

* Corresponding author. Tel.: +91 8895237129; fax: +91 6743060509
E-mail address: snehasis18386@gmail.com (S. Kundu).

central section of open channels as a function of aspect ratio. Yang et al. (2004) analyzed data of Yang (1996) and NHRI (1957) and proposed an empirical model for dip position. This model is verified for a wide range of channel aspect ratio from 4.1 to 15. They found that velocity dip may occur very close to sidewall region even when channel aspect ratio is large. This model is applicable both in wide and narrow open channels and also applicable at the central section of any open channels. Absi (2011) considered this model to predict the velocity-dip-position for validating his proposed velocity model named as full dip-modified-log-wake law (fDMLW-law). Bonakdari et al. (2008) critically analyzed both the models of Wang et al. (2001) and Yang et al. (2004) for small channel aspect ratio. They found that both of these models overestimate the experimental results when Ar is small. On the basis of experimental observation from five researchers, Bonakdari et al. (2008) proposed a sigmoid model for dip position varying Ar . Apart from these empirical and analytical models, researchers proposed numerical models and methods to determine the velocity-dip-position (Wang and Cheng, 2005; Sarma et al., 2000). Guo and Julien (2008) describes a method to determine the dip position by fitting a parabola to the velocity data near the free surface region. Guo (2013) studied the velocity profile for smooth rectangular open channel flows. He found that the velocity-dip-position shifts exponentially from the water surface to half flow depth as the channel aspect ratio decreases from infinity to zero. He proposed an empirical relation between bed shear stress and free surface shear stress based on the experimental data of Hu and Hui (1995) and based on this assumption he proposed an empirical model for dip position at the channel central section. Besides this, Guo (2013) analyzed the models of Wang et al. (2001), Yang et al. (2004) and Bonakdari et al. (2008) and found that none of these models satisfy the asymptotic condition $0.5 \leq \xi_d \leq 1$ consistent with Hu and Hui (1995) observations. Pu (2013) proposed an empirical model for velocity-dip-position at the central section of open channel. This model satisfies both the asymptotic boundary conditions. Pu (2013) validated his model for both wide and narrow open channel flows with rough and smooth beds. Most of these models of velocity-dip-position found in literature are empirically proposed and model parameters are determined from limited number of experimental data and did not satisfy the asymptotic boundary condition $0.5 \leq \xi_d \leq 1$ (Hu and Hui, 1995). The numerical models based on RANS equation create difficulty regarding computational purpose and accuracy of the solutions. Therefore, in this study we applied the entropy theory based approach to develop a model for the velocity-dip-position.

Since the development of the entropy theory by Shannon (1948) and of the principle of maximum entropy (POME) by Jaynes (1957), there has been a number of applications of entropy theory in hydrological and environmental sciences (Singh, 1997; Nourani et al., 2015). Chiu (1987, 1989) has derived the probability density function for velocity and using the POME they derived the models for mean velocity distribution, turbulent shear stress distribution and particle suspen-

sion concentration distribution. Later on, Luo and Singh (2011), Singh and Luo (2011) and Kumbhakar and Ghoshal (2016a, b) studied on velocity distribution in an open channel flow by employing the concept of Tsallis (1988) and Renyi (1961) entropy which are the generalizations of Shannon entropy. However, the present study focuses on the velocity dip-position derived from the Shannon entropy. Chiu and Tung (2002) studied the maximum velocity and regularities in open channel flows and derived an empirical model using regression technique for dip-position which is expressed as:

$$\xi_d = 1 + 0.2 \ln \frac{G(M)}{58.3}, G(M) = \frac{(e^M - 1)^2}{(M - 1)e^M + 1} \quad (1)$$

where M is the entropy parameter (Chiu, 1987). The computation of velocity-dip-position from this model requires the knowledge of M . Chiu and Tung (2002) computed the value of M from the average value $u - u_{\max}$ relation. Therefore, it gives an average relation between ξ_d and M which may indicate that exact value may fluctuate or deviate above or below that proposed relation. Though an explicit model for velocity-dip-position has been developed using the entropy concept, but the computation of dip-position is not straight forward. Besides this, the above model gives the range of dip-position $0.39 \leq \xi_d \leq 1$ which suggests that the lower asymptotic boundary condition is not achieved. Therefore, a more general model for velocity-dip-position in an open channel is still lacking in the literature.

Our motivation for the present study stems from the fact that a mathematical expression of velocity-dip-position throughout the cross section of an open channel based on a theoretical approach is not proposed yet. Though the application of Shannon entropy theory for problems of open channel hydraulics has been extensive, still no direct application has been made by researchers regarding the location of maximum velocity for open channel flow. Therefore, in this study, we make an attempt to derive an entropy based model for velocity-dip-position throughout the cross section of an open channel. The knowledge of dip-position will help to understand the mean velocity distribution over the entire cross section as well as flow dynamics of open channel flow. It will be helpful to the river engineers, researchers dealing with open channel hydraulics and sediment transportation problems and in a number of problems of socio-economic importance like construction of dams, flood control etc.

The organization of our work is as follows. In section 2, we propose the mathematical approach on the basis of Shannon entropy and principle of maximum entropy (POME) developed by Jaynes (1957) for finding dip position. The model for velocity-dip-position for the entire cross section and for the central section is also derived in this section. Section 3 depicts the validation of proposed models by comparing these with a wide range of 23 experimental data available in literature including recent results. The appropriate form of the models for entire cross section and at the central section of

open channel is also mentioned in section 3. To get a quantitative idea about the goodness of fit of the models when compared with other existing models, five statistical parameters (errors) are considered and results are discussed in section 4. In section 5, we discuss the variation of the model with variation of different parameters. Section 6 describes the efficiency of the model and the paper is completed by a conclusion.

2. Entropy-Based Formulation

The location of maximum velocity from channel bed i.e. velocity-dip-position y_d , may or may not be equal to the flow depth. It is established by several investigators that at the central section of a narrow channel $y_d < h$, and of a wide open channel $y_d = h$. Due to the presence of cellular secondary current in a cross sectional plane (Gibson, 1909), the maximum velocity appears at free surface at section 1-1 and it appears below the free surface at section 2-2 (Figure 1). As a consequence, the dip position changes along the cross section. As the distance z from side wall increases, the value of y_d gradually increases from lower value y^* to upper value d^* (where y^* is the location of maximum velocity very close to side wall and d^* is the location of maximum velocity at central section, Figure 2). In case of wide open channel, $d^* = h$ and for narrow open channel $d^* < h$. Therefore, the location of maximum velocity y_d is a function of z and hence one can express dip-position y_d as:

$$y_d = \phi(z) \tag{2}$$

where Φ is some function of z . To investigate the effect of sidewall on location of maximum velocity in open channel flow, Yan et al. (2011) performed a series of experiments. All experiments were conducted in a 12m long and 0.42m wide recirculating rectangular flume with glass sidewalls and over a plastic bed. The slope could be adjusted to obtain uniform flow conditions. The discharge was measured by an acoustic flow meter. The water level was controlled by a tail gate weir and measured by a point gauge meter. The TSI Laser Doppler Velocimeter was utilized to obtain the velocity distribution. The experiments were performed for five different flow depths, $h = 0.06$ m, 0.09 m, 0.12 m, 0.15 m, and 0.18 m and in each case, velocities were measured at different positions from the sidewall. From a statistical analysis of their experimental data, they proposed that the flow field may be divided into two regions: (a) relatively strong sidewall region and (b) relatively weak sidewall region. They also concluded that in the former region, the distance to the sidewall greatly affects the location of maximum velocity and in the latter region, both the distance to the sidewall and the aspect ratio influence the location of the maximum velocity. Therefore, in this study we consider dip position y_d as:

$$y_d = \phi(z, b, h) \tag{3}$$

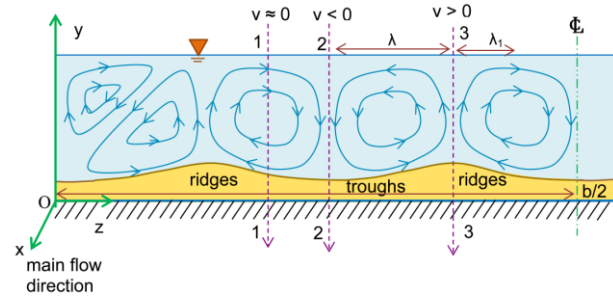


Figure 1. Schematic diagram of secondary current in a cross sectional plane for open channel flow.

Using a dimensional analysis, we can write Equation (3) as:

$$\xi_d = \phi(z/h, b/h) = \phi(z/h, Ar) \tag{4}$$

where $\xi_d = y_d/h$ is the dimensionless height of velocity-dip-position from channel bottom and $Ar = b/h$ is the channel aspect ratio where b denotes the width of the channel. Therefore, ξ_d can be considered as a random variable and has a probability distribution. Following the similar definition for velocity distribution and considering the general form of the cumulative probability distribution proposed by Singh (2011), in this study we assume that the CDF for velocity-dip-position as:

$$F(\xi_d) = P(\text{dip position} \leq \xi_d) = \left(\frac{z}{z_{\max}} \right)^n \tag{5}$$

where $F(\xi_d)$ is the cumulative distribution function, P denotes probability, n is the fitting parameter which describes the declination of the CFD curve and z_{\max} is the maximum value of z . Generally, in a cross sectional plane the flow is symmetrical about the center line. Therefore, the value of ξ_d appears in a symmetrical manner on both sides of the center line. Due to this reason, the maximum value of z is considered as $b/2$ i.e. $z_{\max} = b/2$ as on the other side of the center line $\xi_d(z) = \xi_d(b-z)$. Therefore, the probability density function (PDF) of ξ_d is obtained by differentiating Equation (5) with respect to ξ_d as follows:

$$f(\xi_d) = \frac{dF(\xi_d)}{d\xi_d} = \frac{dF}{dz} \frac{dz}{d\xi_d} = n \left(\frac{z}{z_{\max}} \right)^{n-1} \left(z_{\max} \frac{d\xi_d}{dz} \right)^{-1} \tag{6}$$

The hypothesis that the cumulative distribution function $F(\xi_d)$ changes with z , which is presented in Equation (5), is tested with the experimental data from Yang (1996), NHRI (1957) and Yan et al. (2011). The results are plotted in Figure 3 for all experimental data and the coefficient of regression is obtained as $R^2 = 0.98$. From the figure one can observe that the data points are well described by the cumulative distribution function proposed in Equation (5).

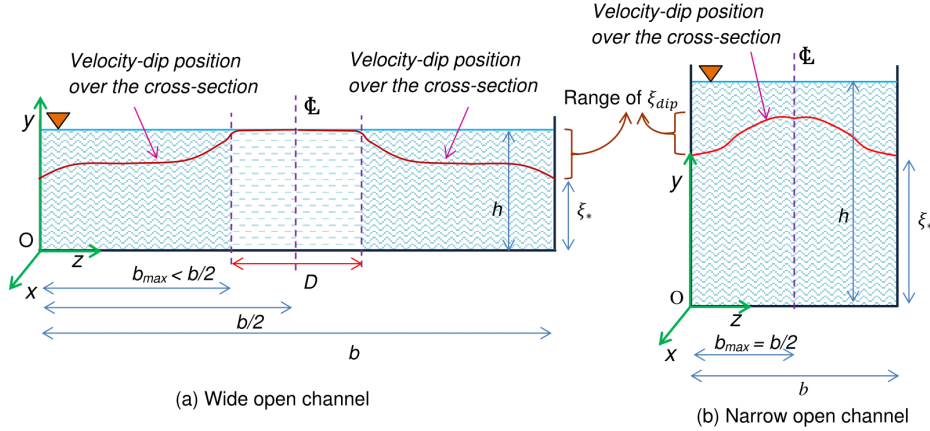


Figure 2. Variation of velocity-dip-position for (a) wide and (b) narrow open channels along a cross sectional plane.

To find the probability density function $f(\xi_d)$ of ξ_d , we have applied the Shannon entropy for velocity-dip position which is given as (Shannon, 1948; Shannon and Weaver, 1949):

$$H(\xi_d) = - \int_{\xi_*}^{D_*} f(\xi_d) \ln[f(\xi_d)] d\xi_d \quad (7)$$

where ξ_* and D_* the lower and upper bounds of ξ_d . Equation (7) defines a measure of uncertainty of the function $f(\xi_d)$. To find $f(\xi_d)$, the principle of maximum entropy (POME) developed by Jaynes (1957, 1982) is applied which includes the specification of certain information called constraints, on velocity-dip-position. According to the POME, to get the least biased probability of the random variable, we maximize the entropy function H subject to some specific constraints.

straints, the total probability law must be satisfied for the probability density function $f(\xi_d)$. Therefore, the first constraint is given as:

$$C_1 = \int_{\xi_*}^{D_*} f(\xi_d) d\xi_d = 1 \quad (8)$$

Generally the other constraint is taken as the mean of ξ_d . But several authors used other different kinds of constraints in their study (Singh, 1998; Singh and Luo, 2011). Therefore, following Singh (1998) and Singh and Luo (2011) to derive the velocity-dip-position model for the present study, the other constraint is taken as:

$$C_2 = \int_{\xi_*}^{D_*} \ln(1 - \xi_d) f(\xi_d) d\xi_d = \overline{\ln(1 - \xi_d)} \quad (9)$$

Equation (9) gives the mean of the logarithmic values of $(1 - \xi_d)$.

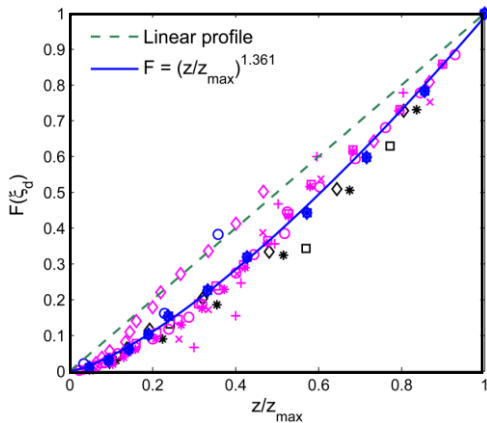


Figure 3. Cumulative probability for $F(\xi_d)$. Black symbols from NHRI (1957), magenta symbols from Yang (1996) and blue symbols from Yan et al. (2011).

2.1. Specifications of Constraints

If the dip-position data are available, one way to express the information is in terms of constraints. To define the con-

2.2. Maximization of Entropy Function

In order to get the least biased probability density function $f(\xi_d)$, the Shannon entropy function given by Equation (7) is maximized by POME subject to the constraints given by Equations (8) and (9). The method of Lagrange multiplier is employed here to maximize the function H . The Lagrange function is given as:

$$L = - \int_{\xi_*}^{D_*} f(\xi_d) \ln[f(\xi_d)] d\xi_d - (\lambda_0 - 1) \left(\int_{\xi_*}^{D_*} f(\xi_d) d\xi_d \right) - \lambda_1 \left(\int_{\xi_*}^{D_*} \ln(1 - \xi_d) f(\xi_d) d\xi_d \right) \quad (10)$$

in which λ_0 and λ_1 are Lagrange multipliers. One can also write

Equation (10) by neglecting integration signs as:

$$L = -f(\xi_d) \ln[f(\xi_d)] - (\lambda_0 - 1)f(\xi_d) - \lambda_1 \ln(1 - \xi_d) f(\xi_d) \tag{11}$$

In order to obtain $f(\xi_d)$ which maximizes L , the Euler-Lagrange equation of calculus of variation has been used. Therefore differentiating L with respect to f (considering f as variable) and equating the derivative $\partial L / \partial f$ to zero one obtains:

$$\frac{\partial L}{\partial f} = 0 = -\ln[f(\xi_d)] - 1 - (\lambda_0 - 1) - \lambda_1 \ln(1 - \xi_d) \tag{12}$$

Rearranging Equation (12), the probability density function $f(\xi_d)$ for velocity-dip-position containing the Lagrange multipliers is expressed as:

$$f(\xi_d) = \exp(-\lambda_0)(1 - \xi_d)^{-\lambda_1} \tag{13}$$

Therefore, the cumulative distribution function $F(\xi_d)$ is obtained as:

$$F(\xi_d) = \int_{\xi_*}^{D_*} f(\xi_d) d\xi_d = \frac{\exp(-\lambda_0)}{\lambda_1 - 1} \left[(1 - \xi_d)^{-\lambda_1 + 1} - (1 - \xi_*)^{-\lambda_1 + 1} \right] \tag{14}$$

One can observe from Equations (13) and (14) that the probability density function and the cumulative distribution function depend on the value of Lagrange multipliers λ_0 and λ_1 . Therefore, determination of these parameters is required which gives the complete understanding of these functions.

2.3. Determination of Lagrange Multipliers

Equations (13) and (14) contain two unknown Lagrange multipliers λ_0 and λ_1 which are determined in the following way. Substitution of Equation (13) into Equation (8) gives:

$$\int_{\xi_*}^{D_*} \exp(-\lambda_0)(1 - \xi_d)^{-\lambda_1} d\xi_d = 1 \tag{15}$$

$$\Rightarrow \exp(\lambda_0) = \frac{(1 - D_*)^{-\lambda_1 + 1} - (1 - \xi_*)^{-\lambda_1 + 1}}{\lambda_1 - 1} \tag{16}$$

$$\Rightarrow \lambda_0 = \ln \left[(1 - D_*)^{-\lambda_1 + 1} - (1 - \xi_*)^{-\lambda_1 + 1} \right] - \ln[\lambda_1 - 1] \tag{17}$$

Equation (17) shows that λ_0 is a function of λ_1 . Therefore, differentiating Equation (17) with respect to λ_1 we get:

$$\frac{\partial \lambda_0}{\partial \lambda_1} = \frac{(1 - D_*)^{-\lambda_1 + 1} \ln(1 - D_*) - (1 - \xi_*)^{-\lambda_1 + 1} \ln(1 - \xi_*)}{(1 - D_*)^{-\lambda_1 + 1} - (1 - \xi_*)^{-\lambda_1 + 1}} - \frac{1}{\lambda_1 - 1} \tag{18}$$

On the other hand, Equation (15) can also be written as:

$$\lambda_0 = \ln \int_{\xi_*}^{D_*} (1 - \xi_d)^{-\lambda_1} d\xi_d \tag{19}$$

Differentiating Equation (19) with respect to λ_1 and applying the Liebnitz rule of differentiation under the integral sign we obtain:

$$\frac{\partial \lambda_0}{\partial \lambda_1} = - \frac{\int_{\xi_*}^{D_*} (1 - \xi_d)^{-\lambda_1} \ln(1 - \xi_d) d\xi_d}{\int_{\xi_*}^{D_*} (1 - \xi_d)^{-\lambda_1} d\xi_d} = - \overline{\ln(1 - \xi_d)} \tag{20}$$

Comparing Equation (18) and Equation (20) and eliminating λ_0 one obtains the equation for λ_1 as:

$$\frac{(1 - D_*)^{-\lambda_1 + 1} \ln(1 - D_*) - (1 - \xi_*)^{-\lambda_1 + 1} \ln(1 - \xi_*)}{(1 - D_*)^{-\lambda_1 + 1} - (1 - \xi_*)^{-\lambda_1 + 1}} - \frac{1}{\lambda_1 - 1} = - \overline{\ln(1 - \xi_d)} \tag{21}$$

Equation (21) contains only one parameter λ_0 and therefore can be solved by any numerical method to find its value. One can observe from Equation (21) that the value of the parameter λ_0 depends on the values of ξ_* , D_* and $\ln(1 - \xi_d)$. Similarly from Equation (17), it can be concluded that the value of the parameter λ_0 also depends on ξ_* , D_* and $\ln(1 - \xi_d)$. In real situation, the value of ξ_* is difficult to measure since it appears very close to the side wall. Hu and Hui (1995) measure the location of maximum velocity close to channel side-wall and found that velocity-dip occurs at 50% of the flow depth from channel bottom. Therefore, following this result $\xi_* \approx 0.5$ is considered in this study. The values of these Lagrange multipliers can be calculated either by any numerical methods or by using least square technique from experimental data.

2.4. Proposed Models

Substituting Equation (16) into Equation (13), the probability density function $f(\xi_d)$ of velocity-dip-position is expressed as:

$$f(\xi_d) = \frac{(\lambda_1 - 1)(1 - \xi_d)^{-\lambda_1}}{(1 - D_*)^{-\lambda_1 + 1} - (1 - \xi_*)^{-\lambda_1 + 1}} \tag{22}$$

Similarly substituting Equation (16) into Equation (14), the cumulative distribution function is obtained as:

$$F(\xi_d) = \frac{(1 - \xi_d)^{-\lambda_1 + 1} - (1 - \xi_*)^{-\lambda_1 + 1}}{(1 - D_*)^{-\lambda_1 + 1} - (1 - \xi_*)^{-\lambda_1 + 1}} \quad (23)$$

To obtain the model for velocity-dip-position ξ_d we compare Equation (5) and Equation (23) which results:

$$\frac{(1 - \xi_d)^{-\lambda_1 + 1} - (1 - \xi_*)^{-\lambda_1 + 1}}{(1 - D_*)^{-\lambda_1 + 1} - (1 - \xi_*)^{-\lambda_1 + 1}} = \left(\frac{z}{z_{\max}} \right)^n \quad (24)$$

After simplification of terms, the entropy based model for the velocity-dip-position is obtained as:

$$\xi_d = 1 - \left[a_0 + a_* \left(\frac{z}{z_{\max}} \right)^n \right]^{1/m} \quad (25)$$

where $m = -\lambda_1 + 1$, $a_0 = (1 - \xi_*)^m$ and $a_* = (1 - D_*)^m - a_0$.

If the lateral distance z from side wall is made dimensionless by flow depth h , Equation (25) reduces to:

$$\xi_d = 1 - \left[a_0 + a_1 \left(\frac{z}{h} \right)^n \right]^{1/m} \quad (26)$$

where $a_1 = a_*(2/Ar)^n$ is a parameter that depends on the aspect ratio of channel. Equation (26) is referred as model M1 in this study. One can observe from Equation (26) that the velocity-dip-position is expressed by a power type model and the proposed model M1 contains two unknown parameter a_0 and a_1 and two exponents m and n . Despite the difficulty of the measurement, the values of the model parameters are calculated from the experimental data by using least square fitting technique. It can be observed that number of unknown parameters is four which is comparatively more than the number of parameters present in other models in several previous studies (Wang et al., 2001; Yang et al., 2004; Bonakdari et al., 2008; Absi, 2011; Guo, 2013). Therefore, we try to reduce the number of parameters in the proposed model. It can be observed from Equation (26) that to compute the values of parameters, the value of the Lagrange multiplier λ_1 is required. Therefore, to find its value, Equation (21) is solved numerically and the value obtained as $\lambda_1 = 1.0458$. This suggests that $\lambda_1 > 1$ and $\lambda_1 \approx 1$ and consequently $1/m = -21.835$. To reduce the number of parameters, we assume that $1/m \rightarrow -\infty$. Therefore, under this assumption, Equation (25) reduces to:

$$\xi_d = 1 - a_2 \exp \left[-a_3 \left(\frac{z}{z_{\max}} \right)^n \right] \quad (27)$$

where $a_2 = a_0^{1/m}$ and $a_3 = a_*/(ma_0)$. If the lateral distance z from side wall is made dimensionless by flow depth h , Equation (27) reduces to:

$$\xi_d = 1 - a_2 \exp \left[-a_4 \left(\frac{z}{h} \right)^n \right] \quad (28)$$

Where $a_4 = a_3(2/Ar)^n$. Equation (28) is referred as model M2 in this study. It can easily be observed from Equation (28) that it contains two unknown parameters a_2 and a_4 and an unknown exponent n . All these model parameters in M2 are calculated from experimental data by using least square fitting method.

At the central section of open channel flows, velocity-dip-position is only affected by the channel aspect ratio Ar (Yan et al., 2011). More precisely if the aspect ratio $Ar \leq Ar_c$ (where Ar_c is the critical aspect ratio (Nezu and Rodi, 1985)) at the central section, the maximum velocity occurs below the free surface; otherwise it appears at the free surface. Therefore, the proposed models are modified in the following way. The model M1 is expressed as:

$$\xi_d = 1 - \left[a_0 + a_5 \left(\frac{z}{b/2} \frac{Ar}{Ar_c} \right)^n \right]^{1/m} \quad (29)$$

where $a_0 = (1 - \xi_*)^m$ and $a_5 = a_*(Ar_c/Ar)^n$. In a similar manner, model M2 is modified as:

$$\xi_d = 1 - a_2 \exp \left[-a_6 \left(\frac{z}{b/2} \frac{Ar}{Ar_c} \right)^n \right] \quad (30)$$

where $a_6 = a_4(Ar_c/Ar)^n$. The location of maximum velocity can be calculated from M1 as well as from M2 if the values of the models parameters are specified. The following section describes the computation of model parameters and the validity of the models M1 and M2 with experimental data.

3. Validation with Data and Comparison with Existing Models

To test the validity of the entropy based proposed models M1 and M2, existing data reported in literature from 23 researchers are considered. All the details of the data sets are given in Table 1. Including all the data sets, the aspect ratio has a wide range from 0.1552 to 15. Proposed models are also compared with the models of Wang et al. (2001), Yang et al. (2004), Bonakdari et al. (2008), Guo (2013) and Pu (2013).

3.1. Validation over the Whole Cross Section

To test the validity of the proposed models M1 (Equation (26)) and M2 (Equation (28)) over the entire cross section,

Table 1. Details of Selected Data Set

Serial no.	Data source	Range of aspect ratio	Data points
1	Murphy (1904)	0.1552 ~ 1.3460	5
2	Gibson (1909)	0.256 ~ 2	5
3	Vanoni (1946)	4.9973 ~ 11.8951	28
4	NHRI (1957)	4.1 ~ 15	24
5	Guy et al. (1966)	7.94 ~ 8.54	6
6	Rajaratnam and Muralidhar (1969)	3.2834 ~ 10.8396	4
7	Knight and Macdonald (1979)	1.0120 ~ 1.012	1
8	Sarma et al. (1983)	2.0240 ~ 7.9835	3
9	Zippe and Graf (1983)	6.1728 ~ 7.6336	5
10	Hu (1985)	1.6642 ~ 11.1319	13
11	Nezu and Rodi (1985)	1.0086 ~ 6.0011	3
12	Coleman (1986)	2.0578 ~ 2.1317	7
13	Nezu and Rodi (1986)	0.1888 ~ 5.42	68
14	Cardoso et al. (1989)	4.6729 ~ 7.3529	5
15	Wang and Qian (1989)	3 ~ 3.75	3
16	Tominaga et al. (1989)	2.0054 ~ 7.9946	3
17	Wang and Fu (1991)	4.1664 ~ 4.2913	4
18	Kironoto and Graf (1994)	2.069 ~ 6.8966	8
19	Song and Graf (1994)	3.0039 ~ 4.5878	12
20	Wang and An (1994)	3.7975 ~ 4.1667	5
21	Yang (1996)	4.47 ~ 9.84	88
22	Larrarte (2006)	1.7562 ~ 2.9248	25
23	Yan et al. (2011)	2.3058 ~ 6.9988	5

experimental data from NHRI (1957), Yang (1996) and Yan et al. (2011) are selected. The values of the model parameters are calculated from experimental data by using Matlab non-linear curve-fit function. From the curve fitting results, the value of parameters for model M1 is obtained as $a_0 = 1.032$, $a_1 = 0.02176$, $n = 1.208$ and $1/m = -21.84$. The R^2 value for this fitting is obtained as 0.80. Similarly, for the model M2, the value of the model parameters are obtained as $a_2 = 0.5005$, $a_4 = 0.4426$ and $n = 1.232$. The R^2 value for this fitting is obtained as 0.8. The results obtained from the proposed models are plotted in Figure 4 together with the all experimental data. From the figure, one can observe that both the proposed models M1 and M2 agrees well with the experimental data throughout the whole cross section of the channel. More precisely, it can be observed that both the models M1 and M2 give almost similar results over the whole cross section. Due to the scatteredness of the data points near the side wall region, in both these models the value of coefficient of regression (numerical value of R^2) is less.

In this study we also compare the proposed models M1 and M2 given by Equations (26) and (28) respectively with the models of Wang et al. (2001) and Yang et al. (2004). The explicit formulas of these models over the whole cross section are shown in Table 2. All these models are plotted in Figure 4 for comparison purpose. To show the results more precisely, all curves are plotted in a semi logarithmic graph paper. From the figure, one can observe that model of Wang et al. (2001) deviates from the experimental data when $z/h > 2$. In the range of z/h between 0.001 to 2, all the models give almost similar results. To get a quantitative idea about the prediction ac-

curacy of these models, five error terms (Mean absolute standard error, Average percentage relative error, Sum of squared relative error, Sum of logarithmic deviation error and Root mean square error) are calculated for all these four models (M1, M2, model of Wang et al. (2001) and model of Yang et al. (2004)) which are discussed in details in the next section. All the calculated values of the errors are shown in Table 2.

3.2. Validation at the Central Section

The validity of the proposed models M1 (Equation (29)) and M2 (Equation (30)) at the central section of open channels are also tested with the existing experimental data in literature. Since at the central section of open channels, dip position is mainly affected by channel aspect ratio (Nezu and Rodi, 1985; Yan et al., 2011), we modify the proposed models. At the central section $z = b/2$ and the models M1 and M2 can be expressed from Equation (29) and Equation (30), respectively as:

$$\xi_d = 1 - \left[a_0 + a_5 \left(\frac{Ar}{Ar_c} \right)^n \right]^{1/m} \tag{31}$$

and

$$\xi_d = 1 - a_2 \exp \left[-a_6 \left(\frac{Ar}{Ar_c} \right)^n \right] \tag{32}$$

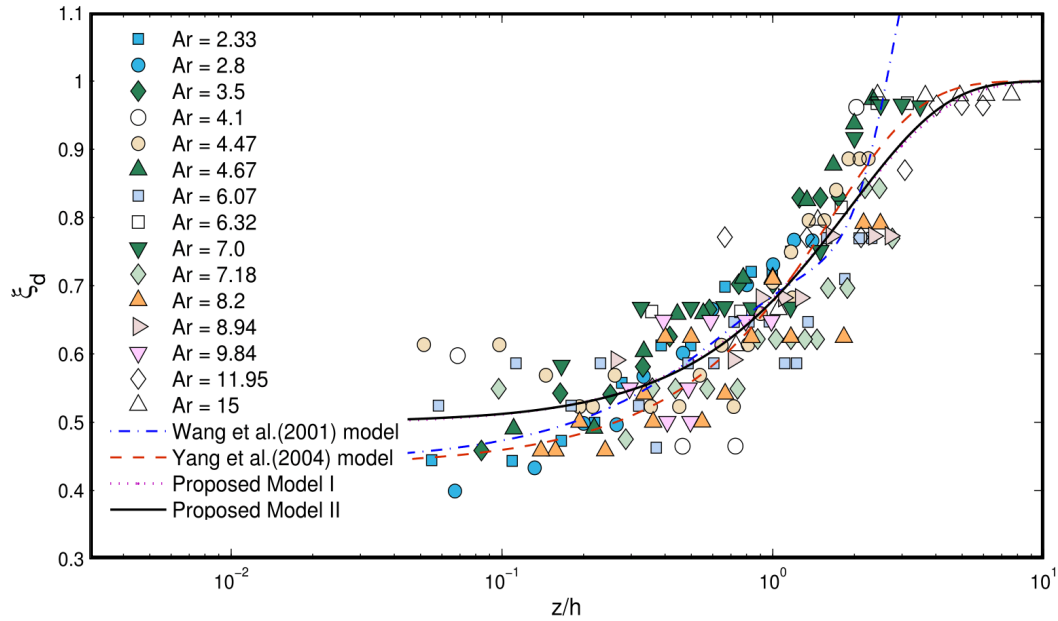


Figure 4. Variation of ξ_d with z/h and validation of entropy based proposed model M1 and M2.

Table 2. Comparison of all Models of Velocity-dip Position Applicable for Entire Cross Section with Experimental Data

No.	Investigators	Proposed formula	Prediction error				
			MASE	r(%)	s ₁	s ₂	RMSE
1	Wang et al. (2001)	$\xi_d = 0.44 + 0.212 \left(\frac{z}{h}\right) + 0.05 \sin \left(\frac{2\pi z}{2.6 h}\right)$	1.1232	11.7696	5.4913	3.8885	0.1564
2	Yang et al. (2004)	$\xi_d = \left[1 + 1.3 \exp \left(-\frac{z}{h}\right)\right]^{-1}$	1.0963	8.8211	2.0854	2.1522	0.0721
3	Kundu and Ghoshal M1 (2016)	$\xi_d = 1 - \left[1.032 + 0.022 \left(\frac{z}{h}\right)^{1.21}\right]^{-21.84}$	1.0893	8.5151	1.8660	1.7450	0.0659*
4	Kundu and Ghoshal M2 (2016)	$\xi_d = 1 - 0.5 \exp \left[-0.443 \left(\frac{z}{h}\right)^{1.232}\right]$	1.0892*	8.5067*	1.8536*	1.7412*	0.0665

* corresponds to minimum error.

Equations (31) and (32) are referred as model M1_c and M2_c respectively in this study. From both the equations, it is observed that the dip position depends on the value of critical aspect ratio Ar_c . Following the study of Nezu and Rodi (1985), in this study $Ar_c \approx 5$ is considered. To find the value of parameters present in the above models, existing experimental data from 21 different experiments are considered (From Hu (1985) to Song and Graf (1994) which are given in Table 1). The values of the parameters are computed by using least square nonlinear curve-fitting technique in Matlab. From the curve fitting results, the value of parameters for model M1_c is obtained as $a_0 = 1.0045$, $a_5 = 0.01228$, $n = 1.265$ and $1/m = 133.9$. The R^2 value for this fitting is obtained as 0.84. Similarly, for the model M2_c, the value of the model parameters

are obtained as $a_2 = 0.495$, $a_6 = 1.678$ and $n = 1.75$. The R^2 value for this fitting is obtained as 0.87. The results for the models M1_c and M2_c for different aspect ratio are plotted in Figure 5. From Figure 5 one can observe that both the models M1_c and M2_c agree well with experimental data for a wide range of channel aspect ratio. Also one can verify from the figure that when $Ar \rightarrow 0$, $\xi_d \rightarrow 0.5$ for M1_c and $\xi_d \rightarrow 0.5$ for M2_c and when $Ar \rightarrow \infty$, both M1_c and M2_c implies $\xi_d \rightarrow 1$. This suggests that model M2_c satisfies both the asymptotic boundary conditions. The scatterness of the data points about the model Equations (31) and (32) in Figure 5, indicate the uncertainty due to measurements errors and other possible factors. The 95% upper and lower confidence limits of ξ_d at a given value of Ar are also shown in the figure.

Table 3. Previous and Present Models on Velocity-dip-position Applicable at the Central Section of any Open Channel

No.	Investigators	Proposed formula	Prediction error				
			MASE	r(%)	s ₁	s ₂	RMSE
1	Wang et al. (2001)	$\xi_d = 0.44 + 0.212 \left(\frac{Ar}{2} \right) + 0.05 \sin \left(\frac{2\pi}{2.6} \frac{Ar}{2} \right)$	1.1356	13.3739	8.2640	5.9303	0.1731
2	Yang et al. (2004)	$\xi_d = \left[1 + 1.3 \exp \left(-\frac{Ar}{2} \right) \right]^{-1}$	1.0804	7.7556	2.5233	2.1966	0.0687
3	Bonakdari et al. (2008)	$\xi_d = \frac{42.4 + Ar^{4.2}}{94.7 + Ar^{4.2}}$	1.1234	10.1513	4.1832	5.2937	0.0980
4	Absi (2011)	$\xi_d = \left[1 + 1.3 \exp \left(-\frac{Ar}{2} \right) \right]^{-1}$	1.0804	7.7556	2.5233	2.1966	0.0687
5	Guo (2013)	$\xi_d = \left[1 + \exp \left\{ -\left(\frac{Ar}{\pi} \right)^{1.5} \right\} \right]^{-1}$	1.0822	7.5499	2.1294	2.2093	0.0699
6	Pu (2013)	$\xi_d = \frac{40.1 + Ar^{4.4}}{80.5 + Ar^{4.4}}$	1.1035	9.5158	3.3958	3.4267	0.0875
7	Kundu and Ghoshal M1 _c	$\xi_d = 1 - \left[1 + 0.013 \left(\frac{Ar}{Ar_c} \right)^{1.265} \right]^{-133.9}$	1.0835	7.7702	2.3037	2.2485	0.0697
8	Kundu and Ghoshal M2 _c	$\xi_d = 1 - 0.495 \exp \left[-1.678 \left(\frac{Ar}{Ar_c} \right)^{1.75} \right]$	1.0791*	7.5028*	2.0298*	2.0847*	0.0664*

* corresponds to minimum error.

Proposed models M1_c and M2_c given by Equation (31) and Equation (32) respectively are also compared with other existing models from Wang et al. (2001), Yang et al. (2004), Bonakdari et al. (2008), Guo (2013) and Pu (2013) at the central section for different aspect ratio of open channels. The explicit forms of the models for all aforementioned researchers are shown in Table 3. All these selected models are plotted in Figure 5 together with model M1_c and M2_c respectively. From the figure it can be observed that the computed values of velocity-dip-position by all these models are comparable to each other. Therefore, to analyze the accuracy of these models, five different error terms (Mean absolute standard error, Average percentage relative error, Sum of squared relative error, Sum of logarithmic deviation error and Root mean square error) are also computed and shown in Table 3. From the table it can be observed that the prediction accuracy of M2_c is superior to other all existing models. This result suggests that dip-position is best described by an exponential decay type model. Therefore, this study not only provides good models for dip-position but also gives a theoretical base which was lacking in the literature till now.

4. Error Analysis

To compare the proposed models M1, M2, M1_c and M2_c with other existing models in literature detail error analysis

has been carried out. Instead of calculating a single error term and determining the result, in this study we consider five different statistical parameters in order to get a vivid idea about the comparison of all the models. These five different statistical quantities are: (i) Mean absolute standard error (MASE), (ii) Average percentage relative error (*r* %), (iii) Sum of squared relative error (*s*₁), (iv) Sum of logarithmic deviation error (*s*₂) and (v) Root mean square error (RMSE). The definitions of these errors are given in details as follows:

(1) Mean absolute standard error (MASE) is defined as:

$$MASE = \frac{1}{N} \sum_{i=1}^N M_i \tag{33}$$

where *M*_{*i*} is given as

$$M_i = \begin{cases} \frac{\xi_{d,c}}{\xi_{d,o}} & \text{if } \xi_{d,c} > \xi_{d,o} \\ \frac{\xi_{d,o}}{\xi_{d,c}} & \text{if } \xi_{d,c} < \xi_{d,o} \end{cases}$$

(2) Average percentage relative error is denoted by *r* and is defined as:

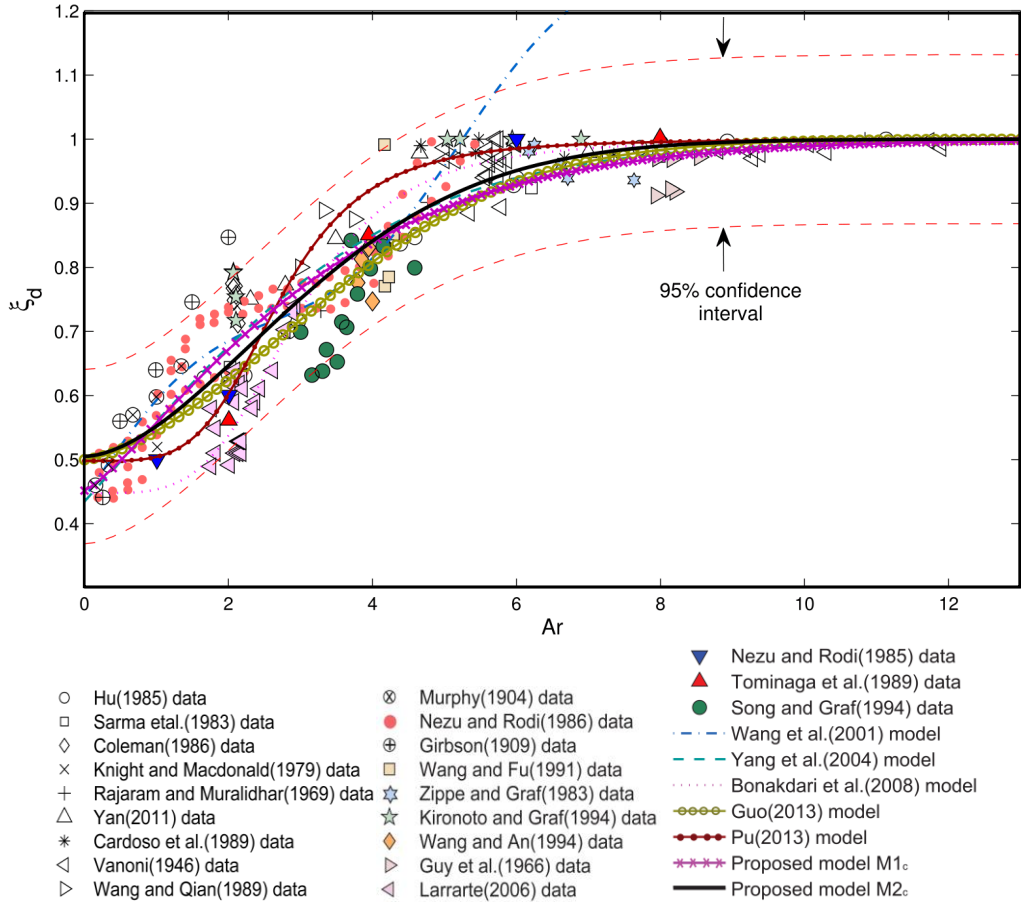


Figure 5. Variation of ξ_d with aspect ratio Ar and validation of proposed model $M1_c$ and $M2_c$ at the central section of open channels.

$$r = \frac{1}{N} \sum_{i=1}^N \frac{|\xi_{d,c} - \xi_{d,o}|}{\xi_{d,o}} \times 100(\%) \quad (34)$$

(3) Sum of squared relative error is denoted by s_1 and is defined as:

$$s_1 = \sum_{i=1}^N \frac{(\xi_{d,c} - \xi_{d,o})^2}{\xi_{d,o}^2} \quad (35)$$

(4) Sum of logarithmic deviation error defined using the logarithmic value of dip position is denoted by s_2 and is expressed as:

$$s_2 = \sum_{i=1}^N (\log |\xi_{d,c}| - \log |\xi_{d,o}|)^2 \quad (36)$$

and

(5) The root mean square error (RMSE) is defined as:

$$RMSE = \sqrt{\frac{1}{N} \sum_{i=1}^N (\xi_{d,c} - \xi_{d,o})^2} \quad (37)$$

where in all these error terms N denotes the total number of data points, $\xi_{d,c}$ and $\xi_{d,o}$ denote the computed and observed values of dimensionless velocity-dip-position respectively.

The computed values of all these errors for the models (detail formulas are given in Table 2) are presented in the Table 2 for all the selected experimental data where star (*) denotes the least error among all these models. From the error results in this table, one can observe that the proposed model M2 has the least average percentage relative error of 8.5067% which gives the best representation of the experimental measurements. From the table it can also be observed that in most of the cases the least value of all these errors corresponds to the model M2. In particular, in spite of less number of parameters than M1 and its simpler form, M2 (Equation (28)) performs even better than all other formulas proposed by Wang et

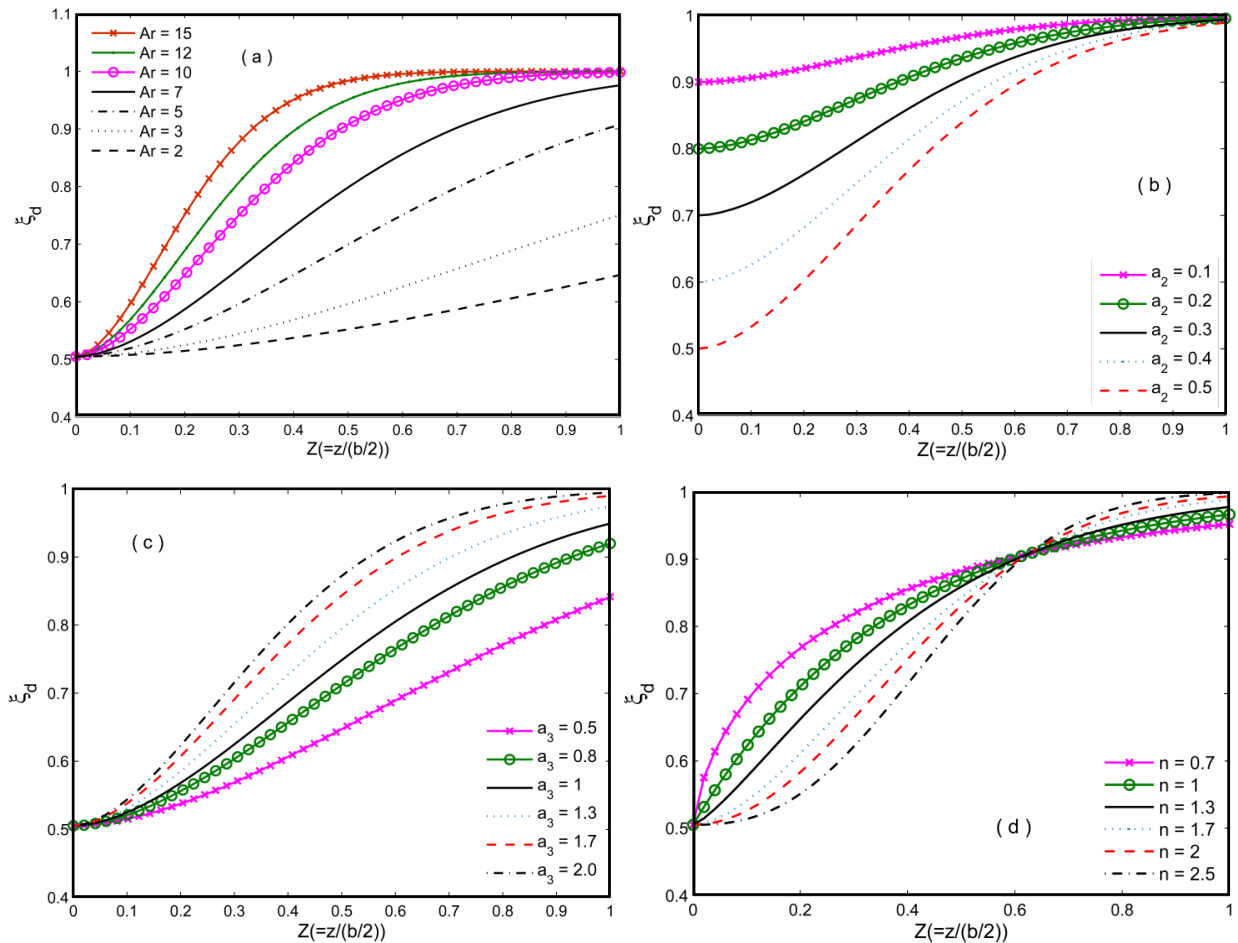


Figure 6. Variation of M2 with model parameters over the half cross section (a) variation with different aspect ratio Ar ; (b) variation with parameter a_2 ; (c) variation with parameter a_3 ; and (d) variation with exponent n .

al. (2001) and Yang et al. (2004) and M1. This comparison results show the superiority of the proposed entropy based model M2.

Similarly, errors for the models for central section of open channel (detail formulas are given in Table 3) are computed and results are shown in Table 3. From the result it can be observed that minimum error corresponds to the proposed model M2_c in this study with the least value of average percentage relative error 7.5028%. The average percentage relative error for the other formulas varies from 7.5499% to 13.3739%. The values of s_1 and s_2 , MASE and RMSE also clearly indicate the best performance of entropy based model M2_c (Equation (32)) compared to other empirical models.

5. Variation of the Model with Change of Parameters

From the comparison results and error analysis in previous two sections, one can find that among two proposed models, M2 gives better result in predicting velocity-dip-position for the entire cross section of any open channel. The

other advantage of this model is that it contains less number of parameters. Therefore, in this section we will discuss the variation of the modified model M2 (Equation (30)) with the change of parameters over the half cross section. The modified Model M2 (Equation (30)) contains three parameters a_2 , a_3 and the exponent n . First the effect of change of aspect ratio on dip position is considered. Thereafter, for a particular value of aspect ratio the variation in dip position with aforementioned parameters are discussed.

Figure 6(a) shows the variation of dip position with the variation of channel aspect ratio. In the figure the change in dip position for seven different values of the aspect ratio $Ar = 2, 3, 5, 7, 10, 12$ and 15 is plotted. The values of other parameters are kept fixed to $a_2 = 0.495$, $a_3 = 1.678$ and $n = 1.75$. From the figure it can be observed that for any fixed value of aspect ratio, ξ_d gradually decreases with decrease of lateral coordinate $Z(=z/(b/2))$. More precisely, when $Ar \leq 7$, the decrease of ξ_d happens gradually and for $Ar > 7$, decrease of ξ_d is not gradual. Furthermore it is also clear from the figure that for higher values of aspect ratio (gene-

rally indicates wide open channel) in the region $0.7 \leq Z \leq 1$, the change in dip position is almost negligible. This indicates that for wide open channels, in a region about the center line, the effect of channel aspect ratio on dip position is almost negligible and flow becomes two-dimensional. These results support the findings of Nezu and Rodi (1985). Figure 6(a) also indicates that at the central section ($Z = 1$), when $Ar \leq 7$ the dip position occurs on or below 90% of the flow depth from channel bed and for $Ar > 7$ no significant dip occurs at the central section.

Figure 6(b) shows the variation of dip position for six different values of parameter a_2 (from 0.1 to 0.5 with an increment of 0.1). Here the value of other parameters are kept fixed at $Ar = 8$, $a_3 = 1.678$ and $n = 1.75$. Figure 6(b) shows that at any fixed position from side wall, the value of ξ_d decreases with increase of a_2 . The deviation of ξ_d for two different values of a_2 gradually increases near the side wall region. Also it can be observed from the figure that at a very close region to side wall, regardless to the value of all other parameters, dip always appears.

In Figure 6(c), the variation of dip position with the variation of parameter a_3 is discussed. The change in ξ_d for six different values of $a_3 = 0.5, 0.8, 1, 1.3, 1.7$ and 2 are plotted in the figure. The value of other parameters are kept fixed at $Ar = 8$, $a_2 = 0.459$ and $n = 1.75$. Figure 6(c) shows that for a fixed value of Z , ξ_d increases with the increase of a_3 . It is also found that at the central section where $Z = 1$, significant dip occurs for $a_3 < 2$ otherwise maximum velocity appears at the free surface.

Similarly, in Figure 6(d) the effect of exponent n on dip position is discussed. In the figure the change of dip for six different values of n is plotted. The value of other parameters are kept fixed at $Ar = 8$, $a_2 = 0.459$ and $a_3 = 1.678$. It is interesting to observe from the figure that in the region $0 \leq Z \leq 0.625$, dip value decreases with increase of n and in the region $0.625 \leq Z \leq 1$, dip value increases with increase of exponent n . In other words, the point $Z = 0.625$ becomes a point of reflection of the curves.

6. Discussion

In this section a critical appraisal of the proposed models developed by using entropy concept has been described. At the central section of open channels, the turbulent shear stress is described as a function of only vertical co-ordinate y which can be expressed as (Yang and McCorquodale, 2004):

$$\frac{\tau_t(y, b/2)}{\tau_{*b}} = -\frac{\overline{u'v'}}{u_*^2} = 1 - \frac{y}{h} + \frac{u(y, z/2)v(y, z/2)}{u_*^2} \quad (38)$$

Equation (38) suggests that turbulent shear stress over the entire water column depends on the mean vertical velocity. A number of studies have been carried out by several scientists and it is widely accepted from the result that vertical velocity in the flow is induced by the secondary currents. A thorough literature about the secondary current can be found in Nezu

and Nakagawa (1993), Wang and Cheng (2006) and Kundu (2015). The proper distribution for turbulent shear stress can be found from Equation (38) if a model for uv is known. Yang et al. (2004) proposed that:

$$\frac{u(y, z/2)v(y, z/2)}{u_*^2} \approx -\alpha_1 \frac{y}{h} \quad (39)$$

where α_1 is a parameter. Inserting Equation (39) into Equation (38) we get the shear stress distribution as:

$$\tau_t(y, b/2) = \tau_{*b} \left(1 - \frac{y}{h} \right) - \alpha_1 \tau_{*b} \frac{y}{h} \quad (40)$$

Guo (2013) envisaged $\alpha_1 \tau_{*b}$ as an ‘‘apparent’’ shear stress τ_1 at the water surface. Like the Reynolds shear stress, τ_1 acts like a shear stress at free surface and it physically implicates momentum transfer by secondary currents near the water surface (Guo, 2013). From the no slip boundary condition at the channel bottom Guo (2013) proposed that $\alpha_1 \leq 1$ and obtained the asymptotic boundary condition $0.5 \leq \xi_d \leq 1$.

From the discussion and error analysis in previous sections, it has been observed that proposed model $M2_c$ gives the best result in the context of matching with the experimental data and providing least errors. In this section, we discuss the asymptotic behavior of our model $M2$ for $Ar \rightarrow 0$ and $Ar \rightarrow \infty$. It has already been pointed out by Guo (2013) that most of the previous empirical models are less adequate in the sense of not preserving the asymptotic boundary conditions i.e. $\xi_d \rightarrow 0.5$ when $Ar \rightarrow 0$ and $\xi_d \rightarrow 1$ when $Ar \rightarrow \infty$. To discuss the asymptotic behavior of model $M2_c$, first we consider that $Ar \rightarrow 0$. Then for $Ar \ll Ar_c$ one can observe that:

$$\exp \left[-a_6 \left(\frac{Ar}{Ar_c} \right)^n \right] \rightarrow 1 \quad (41)$$

which implies from Equation (32) that:

$$\xi_d \rightarrow 1 - a_2 = 1 - 0.495 \approx 0.5 \quad (42)$$

Similarly, as a second case we consider $Ar \rightarrow \infty$. Then $Ar \gg Ar_c$ which implies:

$$\exp \left[-a_6 \left(\frac{Ar}{Ar_c} \right)^n \right] \rightarrow 0 \quad (43)$$

and consequently Equation (32) implies that:

$$\xi_d \rightarrow 1 \quad (44)$$

This suggests that the proposed model $M2_c$ satisfies the asymptotic boundary conditions as proposed by Hu and Hui (1995). It is important to mention herein that interested readers can check in a similar way that proposed model $M1_c$ is satisfying the upper asymptotic boundary condition only. This fact also indicates the superiority of the model $M2_c$ than $M1_c$.

Since the establishment of the velocity-dip-phenomenon, several scientists like Prandtl (1925), Vanoni (1941), Gibson (1909), Karcz (1981), Kinoshita (1967), Nezu and Rodi (1985), Nezu and Nakagawa (1993), Wang and Cheng (2005), Wang and Cheng (2006), Yang et al. (2012) tried to find out the reason behind this phenomenon and it has been widely reported that due to the presence of cellular secondary current in a cross sectional plane, velocity dip occurs. It has also been known that in a wide open channel, the strength of secondary current gradually diminished from sidewall to the central section. Due to the negligible effect of secondary current at central section, flow becomes two dimensional (Vanoni, 1941; Nezu and Rodi, 1985). This fact indicates that the dip-position appears at the free surface when effect of secondary current becomes negligible and it appears below free surface when there is significantly strong secondary current. It can be imagined that a damping factor based on the strength of secondary current is acting which compels the dip position to appear below the free surface. This effect of damping gradually increases from central section towards the sidewall as strength of secondary current gradually becomes important; whereas at the central section of a narrow open channel, the damping is dominant as the effect of secondary current cannot be neglected. From the result of $M2$ plotted in Figure 5 it is clear that the height of dip-position from channel bottom gradually decreases to the value 0.495 at the side wall. Therefore, the model $M2_c$ can be expressed as:

$$\xi_d = 1 - a_2 \Phi(Z, Ar) \tag{45}$$

where

$$\Phi(Z, Ar) = \exp \left[-a_6 \left(Z \frac{Ar}{Ar_c} \right)^n \right] \tag{46}$$

The advantage of this equation is that it gives a physical inset of the real dip phenomenon. The function $\Phi(Z, Ar)$ is introduced here as a “damping factor” and the coefficient a_2 is introduced as “damping coefficient”. The variation of the damping function $\Phi(1, Ar)$ at channel central section is plotted in Figure 7 for different channel aspect ratio. From the figure, one can see that as the aspect ratio increases, the damping gradually disappears at the central section of open channels. This indicates that for wide open channel flows, at the central section there is no damping effect on the location of dip-position and as the channel gradually becomes narrow, the damping appears which shifts the dip-position from channel free surface towards channel bottom. Also it is noticeable from the figure that when $Ar \gg Ar_c$, $\Phi \leq 0.0919$ which implicates that the damping can be neglected at the central section

of wide channels.

Similarly, in Figure 8 the damping function $\Phi(Z, Ar)$ is plotted for $0 \leq Z \leq 1$ i.e. over the half cross section for nine different aspect ratio $Ar = 1, 2, \dots, 9$. From the figure it can be observed that for narrow open channels when $Ar \leq 5$, the damping function having the range from 0.1 to 0.5 which indicates that damping effect cannot be neglected over the whole cross sectional plane of the channel. On the other hand, if the channel becomes wide, for example if $Ar \geq 6$, it can be observed from the figure that there exists a central region about the center line, where the damping effect becomes less than 5% and it can be assumed to be negligible. Vanoni (1941) and Nezu and Rodi (1985) observed the same result in their experiments. It is important to note here that since the change for aspect ratio for narrow and wide open channel is gradual, there always exists a fuzziness of the dip-position as well as a critical aspect ratio value for open channels. This indicates that in case of an open channel having aspect ratio 6 or 7, velocity-dip-phenomenon sill may occur. This conclusion also agrees with the result of Guo (2013) who suggested that two-dimensional flow occurs if $Ar \geq 8$.

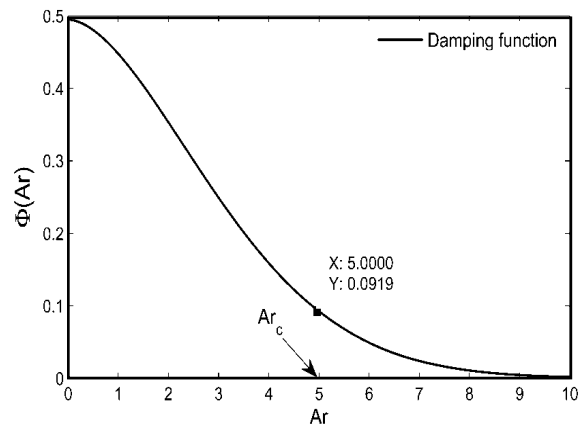


Figure 7. Damping function for different aspect ratio of open channels at the central section.

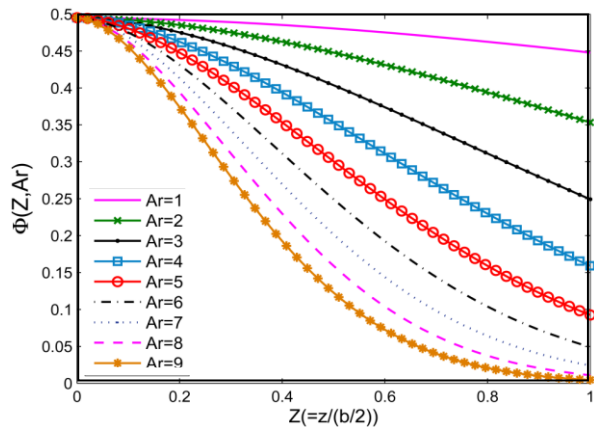


Figure 8. Damping function for different aspect ratio of open channels over the cross section of open channels.

7. Conclusions

Applying the entropy theory based on probability distribution of a random variable and using the principle of maximum entropy, new theoretical models for predicting velocity-dip-position in an open channel flow is derived. The major importance and findings of this study are as follows.

(1) The models have been developed from a theoretical basis rather than proposing them empirically like previous researchers. These models are simple in nature and easy to apply to find the dip-position.

(2) No estimation of parameter is required to find the velocity-dip-position from the proposed models.

(3) The validation of the models by comparing with 23 sets of experimental data shows that models are applicable throughout the whole cross section of any rectangular open channel. It is also found that at the central section of open channels, dip-position changes only with the aspect ratio which is consistent with previous results.

(4) The efficiency of these models are compared with all other existing models in literature by computing five different errors. The obtained results of error analysis show that out of all existing models, proposed models predicts dip-position more accurately over the whole cross section of open channels for a wide range of aspect ratio.

(5) It is also found that out of the two models $M1_c$ and $M2_c$ developed for central section in this study, model $M2_c$ provides best accurate results and satisfies both the asymptotic boundary conditions, whereas the model $M1_c$ only satisfies the upper boundary condition.

(6) Finally, model $M2_c$ is expressed by introducing a damping factor which helps to understand the interrelation between the secondary current and the velocity-dip-position. From the analysis, it is found that at the central section of wide open channels the effect of damping is less than 10% and the effect increases exponentially for narrow open channels.

Nomenclature

a_*, a_i	parameters, $i=1,2,\dots,6$
Ar	channel aspect ratio
Ar_c	critical aspect ratio
b	width of the open channel
C_1, C_2	constraints
D_*	maximum value of ξ_d
f	probability density function (PDF)
F	cumulative distribution function (CDF)
G	a function
H	entropy function
L	Lagrange's function
m	a parameter
M	entropy parameter
n	a parameter
N	total number of data points
P	probability

r	average percentage relative error
s_1	sum of square relative error
s_2	sum of logarithmic deviation error
u	streamwise time mean velocity
u_*	shear velocity
u	streamwise depth mean velocity
u_{max}	streamwise maximum velocity
v	vertical time mean velocity
y	vertical co-ordinate
y_d	location of u_{max} from bed
z	lateral co-ordinate
z_{max}	maximum value of z
Z	dimensionless lateral distance
α_1	a parameter
λ_0, λ_1	Lagrange multipliers
ξ_d	dimensionless dip-position
ξ_*	minimum value of ξ_d
$\xi_{d,c}$	calculated value of ξ_d
$\xi_{d,o}$	observed value of ξ_d
τ_t	turbulent shear stress
τ_{*b}	bed shear stress
τ_1	apparent shear stress
ϕ, Φ	functions

References

- Absi, R. (2011). An ordinary differential equation for velocity distribution and dip-phenomenon in open channel flows. *J. Hydraul. Res.*, 49(1), 82-89. <http://dx.doi.org/10.1080/00221686.2010.535700>
- Bonakdari, H., Larrarte, F., Lassabatere, L., and Joannis, C. (2008). Turbulent velocity profile in fully-developed open channel flows. *Environ. Fluid Mech.*, 8(1), 1-17. <http://dx.doi.org/10.1007/s10652-007-9051-6>
- Cardoso, A.H., Graf, W.H., and Gust, G. (1989). Uniform flow in smooth open channel. *J. Hydraul. Res.*, 27(5), 603-616. <http://dx.doi.org/10.1080/00221688909499113>
- Chiu, C.L. (1987). Entropy and probability concepts in hydraulics. *J. Hydraul. Eng.*, 113(5), 583-599. [http://dx.doi.org/10.1061/\(ASCE\)0733-9429\(1987\)113:5\(583\)](http://dx.doi.org/10.1061/(ASCE)0733-9429(1987)113:5(583))
- Chiu, C.L. (1989). Velocity distribution in open channel flow. *J. Hydraul. Eng.*, 115(5), 576-594. [http://dx.doi.org/10.1061/\(ASCE\)0733-9429\(1989\)115:5\(576\)](http://dx.doi.org/10.1061/(ASCE)0733-9429(1989)115:5(576))
- Chiu, C.L., and Tung, N.C. (2002). Maximum velocity and regularities in open channel flow. *J. Hydraul. Eng.*, 128(4), 390-398. [http://dx.doi.org/10.1061/\(ASCE\)0733-9429\(2002\)128:4\(390\)](http://dx.doi.org/10.1061/(ASCE)0733-9429(2002)128:4(390))
- Coleman, N.L. (1986). Effects of suspended sediment on the open-channel velocity distribution. *Water Resour. Res.* 22(10), 1377-1384. <http://dx.doi.org/10.1029/WR022i10p01377>
- Francis, J.B. (1878). On the cause of the maximum velocity of water flowing in open channels being below the surface. *Trans. ASCE.*, 7(1), 109-113.
- Gibson, A.H. (1909). On the depression of the filament of maximum velocity in a stream flowing through an open channel. *Proc. of the Royal Society A*, 82(553), 149-159. <http://dx.doi.org/10.1098/rspa.1909.0016>
- Gordon, L. (1992). *Mississippi River Discharge*, RD Instruments, San Diego.
- Guo, J. (2013). Modified log-wake-law for smooth rectangular open channel flow. *J. Hydraul. Res.*, 52(1), 121-128. <http://dx.doi.org/10.1080/00221686.2013.818584>

- Guo, J., and Julien, P.Y. (2008). Application of the modified log-wake law in open-channels. *J. Appl. Fluid Mech.*, 1(2), 17-23.
- Guy, H. P., Simons, D.B., and Richardson, E.V. (1966). *Summary of Alluvial Channel Data from Flume Experiments, 1956-1961*, Technical report, United States geological survey water supply, Washington DC.
- Hu, C. (1985). *Effects of Width-to-Depth Ratio and Side Wall Roughness on Velocity Distribution and Friction Factor (in Chinese)*, Master's thesis, Tsinghua University, Beijing, China.
- Hu, C., and Hui, Y. (1995). *Mechanical and Statistical Laws of Open Channel Sediment-Laden Flow (in Chinese)*, Science Press, Beijing.
- Jaynes, E. (1957). Information theory and statistical mechanics: I. *Phys. Rev.*, 106, 620-930. <http://dx.doi.org/10.1103/PhysRev.106.620>
- Jaynes, E. (1982). On the rationale of maximum entropy methods. *Proc. Of IEEE*, 70, 939-952. <http://dx.doi.org/10.1109/PROC.1982.12425>
- Karcz, I. (1981). Reflections on the origin of small scale longitudinal streambed scours. In M. Morisawa (Ed.), *Proc. of the Fourth Annual Geomorphology Symposia Series*, Allen and Unwin, London, pp. 149-177.
- Kinoshita, R. (1967). An analysis of the movement of flood waters by aerial photography: concerning characteristics of turbulence and surface flow (in Japanese). *Photogr. Surv.*, 6, 1-17.
- Kironoto, B.A., and Graf, W.H. (1994). Turbulence characteristics in rough uniform open-channel flow. *Proc. of the ICE: Water Maritime and Energy*, 106(12), 333-344. <http://dx.doi.org/10.1680/iwtme.1994.27234>
- Knight, D.W., and Macdonald, J.A. (1979). Open-channel flow with varying bed roughness. *J. Hydraul. Div.* 105(9), 1167-1183.
- Kumbhakar, M., and Ghoshal, K. (2016a). One dimensional velocity distribution in open channels using renyi entropy. *Stoch. Environ. Res. Risk Assess.*, 1-11, <http://dx.doi.org/10.1007/s00477-016-1221-y>
- Kumbhakar, M., and Ghoshal, K. (2016b). Two dimensional velocity distribution in open channels using renyi entropy. *Physica A Stat. Mech. Appl.*, 450, 546-559. <http://dx.doi.org/10.1016/j.physa.2016.01.046>
- Kundu, S. (2015). *Theoretical Study on Velocity and Suspension Concentration in Turbulent Flow*, Ph.D. Indian Institute of Technology Kharagpur, West Bengal, India.
- Larrarte, F. (2006). Velocity fields in sewers: an experimental study. *Flow Meas. Instrum.*, 17(5), 282-290. <http://dx.doi.org/10.1016/j.flowmeasinst.2006.08.001>
- Luo, H., and Singh, V.P. (2011). Entropy theory for two-dimensional velocity distribution. *J. Hydraul. Eng.*, 16(4), 303-315. [http://dx.doi.org/10.1061/\(ASCE\)HE.1943-5584.0000319](http://dx.doi.org/10.1061/(ASCE)HE.1943-5584.0000319)
- Murphy, C. (1904). Accuracy of stream measurements. *Water Supp. Irrig.*, Paper 95, 111-112.
- Nezu, I., and Nakagawa, H. (1993). *Turbulence in Open-Channel Flows*, A.A. Balkema, Rotterdam, Netherlands.
- Nezu, I., and Rodi, W. (1985). Experimental study on secondary currents in open channel flows. *Proc. of the 21st Congress*, vol. 2, pp. 115-119. IAHR, Madrid.
- Nezu, I., and Rodi, W. (1986). Open-channel flow measurements with a laser dropper anemometer. *J. Hydraul. Eng.*, 112(5), 335-355. [http://dx.doi.org/10.1061/\(ASCE\)0733-9429\(1986\)112:5\(335\)](http://dx.doi.org/10.1061/(ASCE)0733-9429(1986)112:5(335))
- NHRI (1957). *Experimental Study on 3D Velocity Distribution in Smooth Flow*, Nanjing Hydraulic Research Institute, Nanjing, China: National Historic Research Institute (NHRI).
- Nourani, V., Khanghah, T.R., and Baghanam, A.H. (2015). Application of entropy concept for input selection of wavelet-ANN based rainfall runoff modeling. *J. Environ. Inf.*, 26(1), 52-70. <http://dx.doi.org/10.3808/jei.201500309>
- Prandtl, L. (1925). Report on investigations into trained turbulence. *J. Appl. Math. Mech.*, 5, 136-139
- Pu, J.H. (2013). Universal velocity distribution for smooth and rough open channel flows. *J. Appl. Fluid Mech.*, 6(3), 413-423.
- Rajaratnam, N., and Muralidhar, D. (1969). Boundary shear stress distribution in rectangular open channels. *La Houille Blanche*. 24(6), 603-609. <http://dx.doi.org/10.1051/lhb/1969047>
- Renyi, A. (1961). On measures of entropy and information. *Proc. of the 4th Berkeley Symposium on Mathematics, Statistics and Probability*, 1, 547-561
- Sarma, K.V.N., Lakshminarayana, P., and Rao, N.S.L. (1983). Velocity distribution in smooth rectangular open channels. *J. Hydraul. Eng.*, 109, 270-289. [http://dx.doi.org/10.1061/\(ASCE\)0733-9429\(1983\)109:2\(270\)](http://dx.doi.org/10.1061/(ASCE)0733-9429(1983)109:2(270))
- Sarma, K.V.N., Prasad, B.V.R., and Sarma, A.K. (2000). Detailed study of binary law for open channels. *J. Hydraul. Eng.*, 126(3), 210-214. [http://dx.doi.org/10.1061/\(ASCE\)0733-9429\(2000\)126:3\(210\)](http://dx.doi.org/10.1061/(ASCE)0733-9429(2000)126:3(210))
- Shannon, C., and Weaver, W. (1949). *The Mathematical Theory of Communication*. Urbana, Ill: University of Illinois Press.
- Shannon, C.E. (1948). The mathematical theory of communication. *Bell Syst. Tech. J.*, 27, 379-423. <http://dx.doi.org/10.1002/j.1538-7305.1948.tb01338.x>
- Singh, V. P. (1998). Entropy-based parameter estimation in hydrology, Kluwer, Boston.
- Singh, V. P. (1997). The use of entropy in hydrology and water resources. *Hydrol. Process.*, 11(6), 587-626. [http://dx.doi.org/10.1002/\(SICI\)1099-1085\(199705\)11:6<587::AID-HYP479>3.0.CO;2-P](http://dx.doi.org/10.1002/(SICI)1099-1085(199705)11:6<587::AID-HYP479>3.0.CO;2-P)
- Singh, V P., and Luo, H. (2011). Entropy theory for distribution of one-dimensional velocity in open channels. *J. Hydraul. Eng.*, 16(9), 725-735. [http://dx.doi.org/10.1061/\(ASCE\)HE.1943-5584.0000363](http://dx.doi.org/10.1061/(ASCE)HE.1943-5584.0000363)
- Song, T.C., and Graf, W.H. (1994). Non-uniform open channel flow over a rough bed. *J. Hydrosci. Hydraul. Eng.*, 12(1), 1-25.
- Stearns, F.P. (1883). On the current-meter: together with a reason why the maximum velocity of water flowing in open channel is below the surface. *Trans. Am. Soc., Civ. Eng.*, 12(1), 301-338.
- Tominaga, A., Nezu, I., Ezaki, K., and Nakagawa, H. (1989). Three dimensional turbulent structure in straight open channel flows. *J. Hydraul. Res.*, 27(1), 149-173. <http://dx.doi.org/10.1080/00221688909499249>
- Tsallis, C. (1988). Possible generalization of boltzmann-gibbs statistics. *J. Stat. Phys.*, 52(1), 479-487. <http://dx.doi.org/10.1007/BF01016429>
- Vanoni, V.A. (1941). Velocity distribution in open channels. *Civ. Eng.*, 11(6), 356-357.
- Vanoni, V.A. (1946). Transportation of suspended sediment by running water. *Trans. ASCE*, 111, 67-133.
- Wang, X., and An, F. (1994). The fluctuating characteristics of hydrodynamic forces on bed particles. *Int. J. Sediment Res.*, 9(3), 183-192.
- Wang, X., and Fu, R. (1991). Study on the velocity profile equations of suspension flows. *Proc. of the 24th IAHR Congress*, Madrid, Espana, 1991.
- Wang, X., and Qian, N. (1989). Turbulence characteristics of sediment-laden flows. *J. Hydraul. Eng.*, 115(6), 781-799. [http://dx.doi.org/10.1061/\(ASCE\)0733-9429\(1989\)115:6\(781\)](http://dx.doi.org/10.1061/(ASCE)0733-9429(1989)115:6(781))
- Wang, X., Wang, Z., Yu, M., and Li, D. (2001). Velocity profile of sediment suspensions and comparison of log-law and wake-law. *J. Hydraul. Res.*, 39(2), 211-217. <http://dx.doi.org/10.1080/00221680109499822>

- Wang, Z.Q., and Cheng, N.S. (2005). Secondary flows over artificial bed strips. *Adv. Water Resour.*, 28(5), 441-450. <http://dx.doi.org/10.1016/j.advwatres.2004.12.008>
- Wang, Z.Q., and Cheng, N.S. (2006). Time-mean structure of secondary flows in open channel with longitudinal bedforms. *Adv. Water Resour.*, 29(11), 1634-1649. <http://dx.doi.org/10.1016/j.advwatres.2005.12.002>
- Yan, J., Tang, H.W., Xiao, Y., Li, K., and Tian, Z.J. (2011). Experimental study on influence of boundary on location of maximum velocity in open channel flows. *Water Sci. Eng.*, 4(2), 185-191.
- Yang, S.Q. (1996). *Interactions of Boundary Shear Stress, Velocity Distribution and Flow Resistance in 3D Open Channels*, Ph.D. Dissertation, Nanyang Technological University, Singapore.
- Yang, S.Q., and McCorquodale, J.A. (2004). Determination of boundary shear stress and reynolds shear stress in smooth rectangular channel flows. *J. Hydraul. Eng.*, 130(5), 458-462. [http://dx.doi.org/10.1061/\(ASCE\)0733-9429\(2004\)130:5\(458\)](http://dx.doi.org/10.1061/(ASCE)0733-9429(2004)130:5(458))
- Yang, S.Q., Tan, S.K., and Lim, S.Y. (2004). Velocity distribution and dip-phenomenon in smooth uniform open channel flows. *J. Hydraul. Eng.*, 130(12), 1179-1186. [http://dx.doi.org/10.1061/\(ASCE\)0733-9429\(2004\)130:12\(1179\)](http://dx.doi.org/10.1061/(ASCE)0733-9429(2004)130:12(1179))
- Yang, S.Q., Tan, S.K., and Wang, X.K. (2012). Mechanism of secondary currents in open channel flows. *J. Geophys. Res.*, 117 (F4). <http://dx.doi.org/10.1029/2012jf002510>
- Zippe, H.J., and Graf, W.H. (1983). Turbulent boundary-layer flow over permeable and non-permeable rough surfaces. *J. Hydraul. Res.*, 21(1), 51-65. <http://dx.doi.org/10.1080/00221688309499450>